



**HAL**  
open science

## **Anisotropic creep velocity of Dzyaloshinskii domain walls**

Tchilabalo Pakam, Assiongbon Adanlété Adjanoh, Serge Dzo Mawuefa Afenyiveh, Jan Vogel, Stefania Pizzini, Laurent Ranno

► **To cite this version:**

Tchilabalo Pakam, Assiongbon Adanlété Adjanoh, Serge Dzo Mawuefa Afenyiveh, Jan Vogel, Stefania Pizzini, et al.. Anisotropic creep velocity of Dzyaloshinskii domain walls. *Applied Physics Letters*, 2024, 124 (9), pp.092403. 10.1063/5.0191540 . hal-04485390

**HAL Id: hal-04485390**

**<https://hal.science/hal-04485390>**

Submitted on 1 Mar 2024

**HAL** is a multi-disciplinary open access archive for the deposit and dissemination of scientific research documents, whether they are published or not. The documents may come from teaching and research institutions in France or abroad, or from public or private research centers.

L'archive ouverte pluridisciplinaire **HAL**, est destinée au dépôt et à la diffusion de documents scientifiques de niveau recherche, publiés ou non, émanant des établissements d'enseignement et de recherche français ou étrangers, des laboratoires publics ou privés.

# Anisotropic Creep Velocity of Dzyaloshinskii-Moriya Interaction Domain Walls

Tchilabalo Pakam,\* Assiongbon Adanlété Adjanoh, and Serge Dzo Mawuefa Afenyiveh  
*Laboratoire Matériaux, Energies Renouvelables et Environnement, Département de Physique,  
 Faculté des Sciences et Techniques, Université de Kara, 404 Kara, Togo*

Jan Vogel, Stefania Pizzini, and Laurent Ranno  
*Univ. Grenoble Alpes, CNRS, Institut Néel, 38042 Grenoble, France*

(Dated: February 3, 2024)

We have measured the field-driven velocity of chiral Néel domain walls (DWs) stabilized by the Dzyaloshinskii-Moriya interaction (DMI) in a Pt/Co/Ta/Pt film with perpendicular magnetic anisotropy. A simple model based on the universal creep theory allows us to describe the anisotropic propagation of a DW along the contour of a bubble domain, driven by an out-of-plane field in the presence of a static in-plane field. This model is used to obtain the DMI constant from the measurement of the DW propagation with only one value of the in-plane field, simplifying the existing method relying on several measurements. The DMI constant extracted from the model is in good agreement with independent measurements.

The manipulation of spin textures such as domain walls (DWs) does not only rely on the application of a magnetic field. Spin polarized electric currents [1] or more recently pure spin currents [2–4] have been shown to efficiently drive DWs. At the same time, beyond the well-known interface magnetic anisotropy generated in ultra-thin films, an interface-induced non collinear exchange, the Dzyaloshinskii-Moriya interaction (DMI) that stabilizes homochiral domain walls, can sometimes be evidenced when the magnetic system lacks inversion symmetry [5, 6]. Brillouin Light Scattering is one of the few direct methods to obtain the DMI amplitude  $D_i$  [7, 8]. More often the DMI is estimated from evaluating the effective DMI field it generates, through the measurement of the anisotropic propagation of DWs [9].

In this work we provide a description of DW velocity of a circular magnetic domain driven by an out-of-plane magnetic field  $H_z$  in the presence of an in-plane magnetic field  $H_x$ . The determination of  $D_i$  is based on the classical model proposed by Je et al. [9], who showed that the presence of  $H_x$  modifies the DW energy and therefore the DW velocity in the creep regime. An  $H_x$  field with a component parallel/antiparallel to the DW magnetization direction will decrease/increase the DW energy and increase/decrease the DW velocity. In the presence of Néel walls stabilized by DMI, an anisotropic DW propagation is therefore expected. The DW velocity is shown to reach a minimum when  $H_x = H_{DMI}$ , where  $\mu_0 H_{DMI} = \frac{D_i}{M_s \Delta}$  is the effective field that stabilizes Néel walls.  $\Delta$  is the domain wall parameter and  $M_s$  the spontaneous magnetization. Experimentally, this method involves measuring DW velocities along the  $H_x$  direction for a range of  $H_x$  field values, up to fields evidencing a velocity minimum. More recently, Hartmann et al. [10] developed a more complex model for measur-

ing  $H_{DMI}$ . This requires a detailed domain wall energy calculations and does not predict the minimum velocities for  $H = H_{DMI}$ .

We propose a simple analytic model that describes the velocity profiles of the DWs as a function of their polar orientation  $\theta$  in the plane. We then use this model to extract the DMI amplitude from the domain expansion with a single value of the applied field  $H_x$ .

Domain wall dynamics is well described using the Landau-Lifschitz-Gilbert (LLG) equation. This equation is implemented in micromagnetic models using a finite element description of the domains and domain walls. A more compact and analytical model is the  $q - \phi$  model, which describes the domain wall as a rigid spin texture, where only the position  $q$  and the magnetization orientation  $\phi$  in the DW center are time-dependent parameters. This model has been applied to describe the thermally activated creep regime as well as the flow and precessional regimes at larger fields [11]. The  $q - \phi$  model can be extended to include the DMI contribution.

In the presence of defects, in the creep regime, in 2D geometry (thin films), the domain wall velocity follows a universal law, with an exponential field dependence characterized by a critical exponent  $\frac{1}{4}$  (eq.1) [12–14]. At constant temperature, the equation can be written in a more compact form introducing  $\alpha$  and  $v_0$ .

$$\begin{aligned} v(H_z) &= v_d e^{-\frac{kT_d}{kT} \left( \frac{H_z}{H_d} \right)^{-1/4} - 1} \\ v(H_z) &= v_0 e^{-\alpha H_z^{-1/4}} \end{aligned} \quad (1)$$

where  $T_d$ ,  $H_d$  are the characteristic depinning temperature and field and  $v_d$  is the DW velocity at depinning field.

The presence of an in-plane field  $H_x$  can be included in Eq. 1, considering that the coefficient  $\alpha$  depends on the  $H_x$  field only *via* the domain wall energy  $\sigma(H_x)$  [9]:

$$v(H_x, H_z) = v_0 e^{-\alpha \left( \frac{\sigma(H_x)}{\sigma(0)} \right)^{1/4} H_z^{-1/4}} \quad (2)$$

\* Authors to whom correspondence should be addressed:  
 [T. Pakam, pakamtchilaba@gmail.com; S. Pizzini, stefania.pizzini@neel.cnrs.fr]

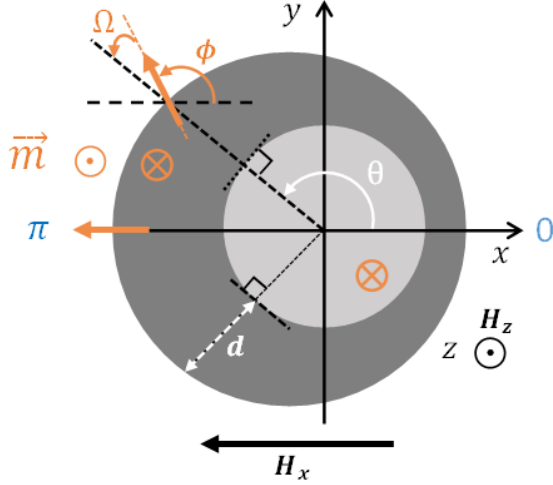


FIG. 1. Schematic representation of the expanding circular magnetic domain driven by an out-plane field ( $H_z$ ) pulse in the presence of an in-plane field ( $H_x$ ) and DMI. In light gray, the first circular domain nucleated with  $H_z$  (with  $H_x=0$ ) and in dark grey, the domain after propagation. The propagation direction of the DW is defined by  $\theta$ , the angle between the DW normal of the first domain and the in-plane field direction. Magnetic moments  $\vec{m}$  within the DW are represented as orange arrows.  $\vec{m}$  is characterized by the angle  $\phi$  with respect to the direction of  $H_x$ .

For a circular domain we define the angles  $\theta$  and  $\phi$  with respect to the in-plane field  $H_x$ :  $\theta$  represents the domain wall propagation direction and  $\phi$  the magnetization direction inside the DW (Fig. 1).  $\Omega = \theta - \phi$  will give the Néel/Bloch character for the wall (Néel DW for  $\Omega = 0, \pi$ , Bloch DW for  $\Omega = \pm\pi/2$ ).

The domain wall energy  $\sigma(H_x, \theta)$  can be obtained by minimizing the different terms that contribute to it; the Bloch term, the DMI term, the Zeeman term associated to the  $H_x$  field and the demagnetizing term associated to the volume charges due to its Néel character:

$$\begin{aligned} \sigma(H_x, \theta, \phi) = & 4\sqrt{AK_{eff}} - \pi|D_i| \cos(\Omega) \\ & - \pi\Delta M_s \mu_0 H_x \cos(\phi) + \frac{\ln(2)}{\pi} t \mu_0 M_s^2 \cos^2(\Omega) \end{aligned} \quad (3)$$

where  $A$  is the exchange constant,  $K_{eff}$  the effective anisotropy,  $D_i$  the DMI constant,  $\Delta = \sqrt{A/K_{eff}}$  domain wall parameter,  $t$  the thickness of the magnetic layer and  $M_s$  its spontaneous magnetization [15–17].

For each  $\theta$  and a given value of  $D_i$ , the minimization of  $\sigma(H_x, \theta)$  gives the equilibrium value of  $\phi$ . The DW velocity  $v(H_x, H_z, \theta)$  can then be obtained using Eqs. 2.

In the rest of our work, we will compare this model (Eq.2) with the experimental velocities and its correctness at determining the DMI amplitude. Firstly, we will describe the experimental protocol used to generate the  $v(H_x, \theta)$  data. Secondly, we will analyze the experimental velocities with the theoretical model.

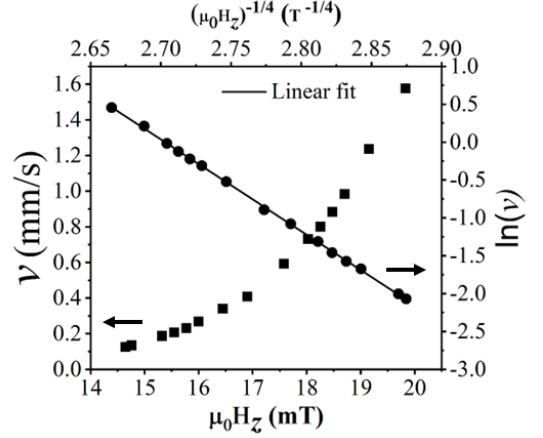


FIG. 2. Plot of the experimental domain wall velocity in the creep regime:  $v$  vs.  $\mu_0 H_z$  (black squares) and  $\ln(v)$  vs.  $(\mu_0 H_z)^{-1/4}$  (black circles) together with the linear fit (black line) to Eq. 1.

The sample Pt(4nm)/Co(0.8nm)/Ta(0.32nm)/Pt(2nm) is deposited by DC magnetron sputtering on Si/SiO<sub>2</sub> substrate with 3 nm of Ta buffer layer. The magnetic characterization is performed using polar Magneto-optical Kerr Effect Microscopy (PMOKE) and Superconducting Quantum Interference Device - Vibrating Sample Magnetometer (SQUID-VSM). The quasi-static parameters are collected in Table I.  $K_{eff}$  was obtained using  $A=16$  pJ/m, value used in the literature for Co layers with similar thicknesses [18]. The DW propagation regime is verified by measuring DW velocities  $v$  as a function of out-of-plane magnetic field ( $H_z$ ). Fig. 2 shows the velocity plot as a function of  $H_z$ . On the figure are plotted simultaneously  $v$  vs.  $H_z$  and  $\ln(v)$  vs.  $H_z^{-1/4}$ . The linear dependence of  $\ln(v)$  with  $H_z^{-1/4}$  proves that DWs in this range of applied field propagate in the creep regime. The creep parameters  $v_0$  and  $\alpha$  are extracted from the fit to Eq. 1 and are:  $v_0 = (1 \pm 0.3) 10^{11} \text{m/s}$  and  $\alpha = (12 \pm 1) T^{1/4}$ . The maximum amplitude of  $\mu_0 H_z$  used for the measurement is 16.5 mT. This value leaves the DW propagation in the creep regime.

Domain imaging is performed using PMOKE microscopy. The protocol starts with the saturation of the magnetization in the out-of-plane direction by applying

TABLE I. Sample quasi-static parameters.  $M_s$  is the spontaneous magnetization,  $K_{eff}$  the effective magnetic anisotropy constant,  $\Delta$  is the DW parameter and  $D_i$ , the DMI strength.

$M_s$	$A$	$K_{eff}$	$\Delta$	$D_i$
MA/m	pJ/m	kJ/m <sup>3</sup>	nm	mJ/m <sup>2</sup>
1.2	16	339	4.4	$-0.43 \pm 0.05$

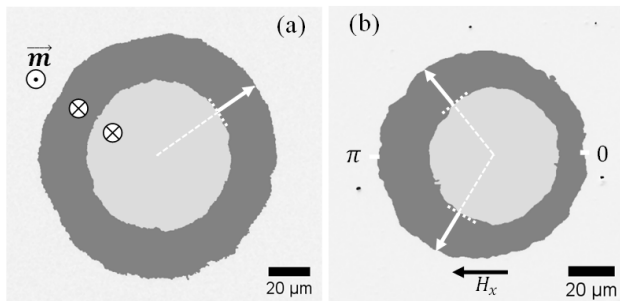


FIG. 3. Differential MOKE image representing the propagation of a DW driven by an out-of-plane magnetic field pulse  $\mu_0 H_z = 16.5 \text{ mT}$  with  $H_x = 0$  (a) and in the presence of an in-plane field  $\mu_0 H_x = 43 \text{ mT}$  (b). In light gray is the first nucleated domain and in dark gray the propagated domain.

a  $H_z$  pulse larger than the saturation field. An opposite  $H_z$  field pulse is then applied to nucleate a circular magnetic domain. The corresponding image is recorded as image 1. The last step of the recording measurement consists in propagating the previously nucleated domain with a pulse of  $H_z$  in the presence or not of a constant and uniform in-plane field  $H_x$ . The image corresponding to this step is recorded as image 2. The images are then processed using the OpenCv(Cv2) Python library [19]. Image 2 is subtracted from image 1. Fig. 3 shows the differential MOKE images measured without in-plane field (a) and with  $\mu_0 H_x = 43 \text{ mT}$  (b). Next, the contours (representative of the DW positions) of the two domains are extracted using contour detection modules. The displacement of the DWs from the contour of the initial domain to the contour of the propagated domain is then used to determine the displacement  $d(\theta)$ . It should be noted that the first domain being circular, the normal to its surface is characterised by the angle  $\theta$ . The DW velocity  $v(H_x, \theta)$  is then extracted from the displacement  $d(\theta)$  during the duration  $dt$  of the field pulse  $H_z$ , from the relation  $d(\theta) = v(\theta)dt$ .

When  $H_x = 0$ , the displacement should be isotropic. To confirm this, we measured the velocity along the entire contour of the magnetic domain. We have defined  $\theta$  with respect to the positive x-direction passing through the center of the nucleated domain. On Fig. 4,  $v(H_x = 0, \theta)$  evidences this isotropic velocity. The isotropic propagation also confirms that  $H_z$  is well aligned and has negligible IP component. This is useful in the analysis of DWs expansion in the presence of the IP field.

Applying an in-plane field leads to an anisotropic propagation of the DWs, highlighting the presence of DMI. The velocity in this case depends on the strength of  $H_x$  and the propagation angle,  $v(H_x, \theta)$ . Fig. 4 represents the velocity profiles for different  $H_x$  values from 0 to 66 mT. For this study, we limited the maximum  $H_x$  value to 66 mT, for two reasons: first, for higher field the density of nucleated domains increases and an overlap between domains can appear; secondly, this prevents temperature

rise due to electromagnets heating. In this limit, the precision of all the used  $H_x$  fields is estimated to be 3mT.

Let us now check the agreement between the theoretical model and the experimental data. The theoretical model describes  $v(H_x, \mu_0 H_z = 16.5 \text{ mT}, \theta)$ . Using a guess value of  $D_i$  (in our case the one obtained in Ref. [18] for a sample with similar composition) the DW energy  $\sigma$  is minimized, numerically, resulting in an equilibrium value for  $\phi$  for each angle  $\theta$ . The resulting  $\sigma$  is then injected into Eq. 2 to obtain the DW velocity profile versus  $\theta$ .  $v_0$  and  $\alpha$  are those deduced from the fit of the experimental velocities to the creep law (Eq. 1). Each  $v(\theta, H_x)$  profile corresponding to a given  $H_x$ , is then fitted by leaving both  $\phi$  and  $D_i$  as free parameters. As can be seen in Fig. 4, the fits are all in good agreement with the data. The model describes correctly not only the minimum and maximum speeds but also the shape of the velocity curve as a function of the polar angle  $\theta$ .

Fitting the full  $v(\theta)$  curve reduces the fitting error compared to fitting only velocities in the  $\theta = 0$  and  $\pi$  directions (along  $\vec{H}_x$ ). The value of the DMI amplitude obtained from the fits of the experimental velocity curves depends very slightly on the  $H_x$  strength. The average value of  $D_i$  is  $-0.43 \pm 0.05 \text{ mJ/m}^2$  giving an average  $H_{DMI}$  field of  $83 \pm 3 \text{ mT}$  (Figure 5(a)). This DMI value is very close to that found in Ref. [18] for a very similar sample composition. On the other hand, since in our sample Ta is only a very thin dusting layer,  $D_i$  is smaller than the values found in the literature for Pt/Co/Ta trilayers with larger Ta layers [20].

This  $H_{DMI}$  value can be compared with that obtained with the classical method proposed by Je et al. [9]. The DWs velocity at  $\theta = 0$  measured as a function of the strength of  $H_x$  is shown in Fig. 5(b). From the fit of the curve using Eq. 3, the DMI field, corresponding to the  $H_x$  with the minimum speed, is determined to be  $\mu_0 H_{DMI} = 84 \pm 5 \text{ mT}$ . This is in excellent agreement with the value obtained from the  $v(\theta)$  fit.

In conclusion, we have proposed a method to extract the DMI value from the analysis of the anisotropic propagation of Néel domain walls as a function of their polar orientation. A simple analytic model based on the universal creep model, allows describing the measured velocity profiles. The DMI amplitudes do not depend on the applied in-plane field and agree with the value extracted from the classical minimum velocity model. The advantage of this protocol is that it allows determining the DMI constant from the velocity measurement with a single  $H_x$  field. This method can be helpful in the case of large  $H_{DMI}$  fields difficult to reach experimentally, or in samples with small anisotropy where large in-plane fields give rise to a large density of nucleated domains.

The authors acknowledge the financial support of Service de coopération et d'action culturelle-France au Togo (SCAC-Togo). We are also thankful to Eric Mossang for his assistance with XRD and XRR measurements, to Philippe David and David Barral for

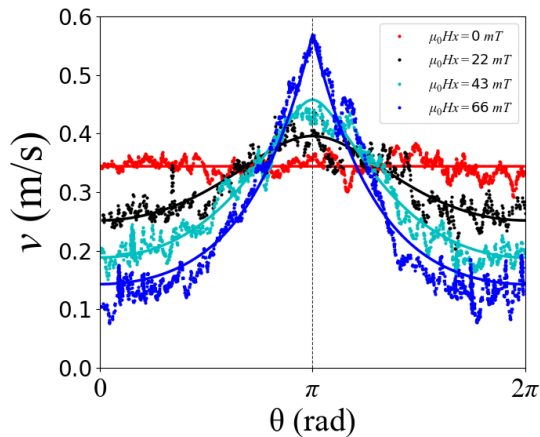


FIG. 4. Anisotropic DW velocity profiles measured for  $\mu_0 H_z = 16.5$  mT with a range of in-plane field  $H_x$  (0 mT, 22 mT, 43 mT and 66 mT) and best fits obtained using the the model  $v(\theta, H_x, \mu_0 H_z = 16.5$  mT).

their assistance for sputtering deposition and fruitful discussions.

- 
- [1] L. Berger, “Exchange interaction between ferromagnetic domain wall and electric current in very thin metallic films,” *Journal of Applied Physics* **55**, 1954–1956 (1984).
- [2] I. M. Miron, T. Moore, H. Szambolics, L. D. Buda-Prejbeanu, S. Auffret, B. Rodmacq, S. Pizzini, J. Vogel, M. Bonfim, A. Schuhl, and G. Gaudin, “Fast current-induced domain-wall motion controlled by the Rashba effect,” *Nature Materials* **10**, 419–423 (2011).
- [3] S. Emori, U. Bauer, S.-M. Ahn, E. Martinez, and G. S. D. Beach, “Current-driven dynamics of chiral ferromagnetic domain walls,” *Nature Materials* **12**, 611–616 (2013).
- [4] K.-S. Ryu, L. Thomas, S.-H. Yang, and S. Parkin, “Chiral spin torque at magnetic domain walls,” *Nature Nanotechnology* **8**, 527–533 (2013).
- [5] I. Dzialoshinskii, “Thermodynamic theory of weak ferromagnetism in antiferromagnetic substances,” *Soviet Physics JETP* **5**, 1259–1272 (1957).
- [6] T. Moriya, “Anisotropic Superexchange Interaction and Weak Ferromagnetism,” *Physical Review* **120**, 91–98 (1960).
- [7] H. T. Nembach, J. M. Shaw, M. Weiler, E. Jué, and T. J. Silva, “Linear relation between Heisenberg exchange and interfacial Dzyaloshinskii–Moriya interaction in metal films,” *Nature Physics* **11**, 825–829 (2015).
- [8] K. Di, V. L. Zhang, H. S. Lim, S. C. Ng, M. H. Kuok, J. Yu, J. Yoon, X. Qiu, and H. Yang, “Direct Observation of the Dzyaloshinskii–Moriya Interaction in a Pt/Co/Ni Film,” *Physical Review Letters* **114**, 047201 (2015).
- [9] S.-G. Je, D.-H. Kim, S.-C. Yoo, B.-C. Min, K.-J. Lee, and S.-B. Choe, “Asymmetric magnetic domain-wall motion by the Dzyaloshinskii–Moriya interaction,” *Physical Review B* **88**, 214401 (2013).
- [10] D. M. F. Hartmann, R. A. Duine, M. J. Meijer, H. J. M. Swagten, and R. Lavrijsen, “Creep of chiral domain walls,” *Physical Review B* **100**, 094417 (2019).
- [11] A. Thiaville and Y. Nakatani, “Domain-Wall Dynamics in Nanowires and Nanostrips,” in *Spin Dynamics in Confined Magnetic Structures III*, Topics in Applied Physics, edited by B. Hillebrands and A. Thiaville (Springer, Berlin, Heidelberg, 2006) pp. 161–205.
- [12] S. Lemerle, J. Ferré, C. Chappert, V. Mathet, T. Giamarchi, and P. Le Doussal, “Domain wall creep in an Ising ultrathin magnetic film,” *Physical review letters* **80**, 849 (1998).
- [13] V. Jeudy, A. Mougin, S. Bustingorry, W. Savero Torres, J. Gorchon, A. B. Kolton, A. Lemaitre, and J.-P. Jamet, “Universal Pinning Energy Barrier for Driven Domain Walls in Thin Ferromagnetic Films,” *Physical Review Letters* **117**, 057201 (2016).
- [14] V. Jeudy, R. Díaz Pardo, W. Savero Torres, S. Bustingorry, and A. B. Kolton, “Pinning of domain walls in thin ferromagnetic films,” *Physical Review B* **98**, 054406 (2018).
- [15] A. Thiaville, S. Rohart, É. Jué, V. Cros, and A. Fert, “Dynamics of Dzyaloshinskii domain walls in ultrathin magnetic films,” *EPL (Europhysics Letters)* **100**, 57002 (2012).
- [16] M. Heide, G. Bihlmayer, and S. Blügel, “Dzyaloshinskii–Moriya interaction accounting for the orientation of magnetic domains in ultrathin films: Fe/W(110),” *Physical Review B* **78**, 140403 (2008).
- [17] J. P. Pellegren, D. Lau, and V. Sokalski, “Dispersive Stiffness of Dzyaloshinskii Domain Walls,” *Physical Review Letters* **119**, 027203 (2017).
- [18] J. P. Garcia, A. Fassatoui, M. Bonfim, J. Vogel, A. Thiaville, and S. Pizzini, “Magnetic domain wall dynamics in the precessional regime: Influence of the Dzyaloshinskii–Moriya interaction,” *Physical Review B* **104**, 014405 (2021).
- [19] I. Culjak, D. Abram, T. Pribanic, H. Dzapov, and M. Cifrek, “A brief introduction to OpenCV,” in *2012 Proceedings of the 35th International Convention MIPRO* (2012) pp. 1725–1730.
- [20] M. Kuepferling, A. Casiraghi, G. Soares, G. Durin,

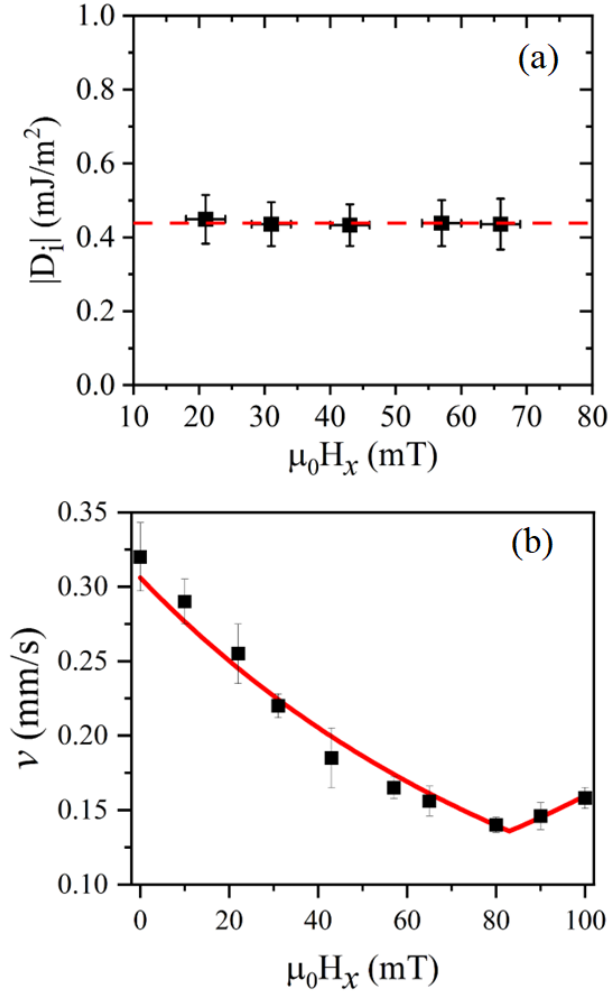


FIG. 5. (a) DMI constant  $D_i$  found from the fit of the experimental curves using Eq. 2, for different values of  $H_x$  (22mT, 32mT, 43mT, 56mT and 66mT). The red dash-line present the average of  $D_i$ ; (b) DW velocity measured as a function of  $H_x$  for  $\theta=0$  with  $\mu_0 H_z=16.5$  mT

F. Garcia-Sanchez, L. Chen, C. H. Back, C. H. Marrows, S. Tacchi, and G. Carlotti, "Measuring interfacial Dzyaloshinskii-Moriya interaction in ultrathin magnetic films," *Reviews of Modern Physics* **95**, 015003 (2023).